Extended Data:

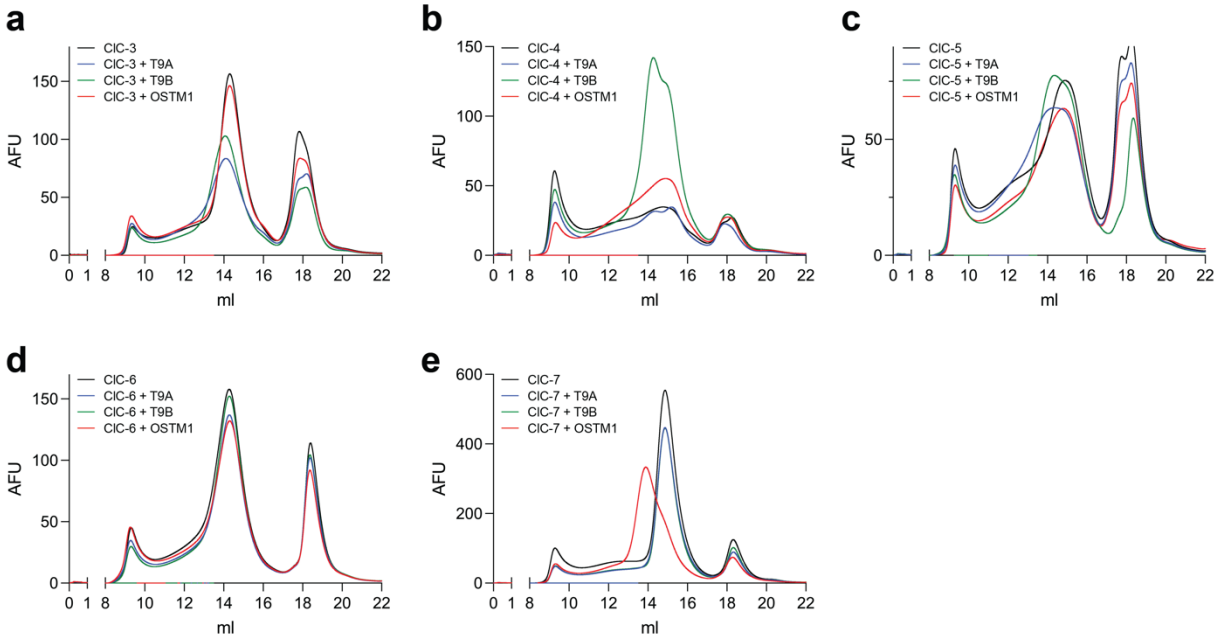

Extended Data Figure 1: T9A and T9B form complexes with ClC-3, ClC-4 and ClC-5. Expi293F cells were transfected with different DNA constructs. After protein purification, the fluorescence of mCerulean-tagged protein was monitored at an excitation/emission wavelength of 433/475 nm, respectively.

(**a**) FSEC profiles of mCerulean-ClC-3 (black), mCerulean-ClC-3 co-expressed with mVenus-T9A (blue), mCerulean-ClC-3 co-expressed with mVenus-T9B (green), and mCerulean-ClC-3 co-expressed with mVenus-OSTM1 (red).

(**b**) FSEC profiles of mCerulean-ClC-4 (black), mCerulean-ClC-4 co-expressed with mVenus-T9A (blue), mCerulean-ClC-4 co-expressed with mVenus-T9B (green), and mCerulean-ClC-4 co-expressed with mVenus-OSTM1 (red).

(**c**) FSEC profiles of mCerulean-ClC-5 (black), mCerulean-ClC-5 co-expressed with mVenus-T9A (blue), mCerulean-ClC-5 co-expressed with mVenus-T9B (green), and mCerulean-ClC-5 co-expressed with mVenus-OSTM1 (red).

(**d**) FSEC profiles of mCerulean-ClC-6 (black), mCerulean-ClC-6 co-expressed with mVenus-T9A (blue), mCerulean-ClC-6 co-expressed with mVenus-T9B (green), and mCerulean-ClC-6 co-expressed with mVenus-OSTM1 (red).

(**e**) FSEC profiles of mCerulean-ClC-7 (black), mCerulean-ClC-7 co-expressed with mVenus-T9A (blue), mCerulean-ClC-3 co-expressed with mVenus-T9B (green), and mCerulean-ClC-7 co-expressed with mVenus-OSTM1 (red).

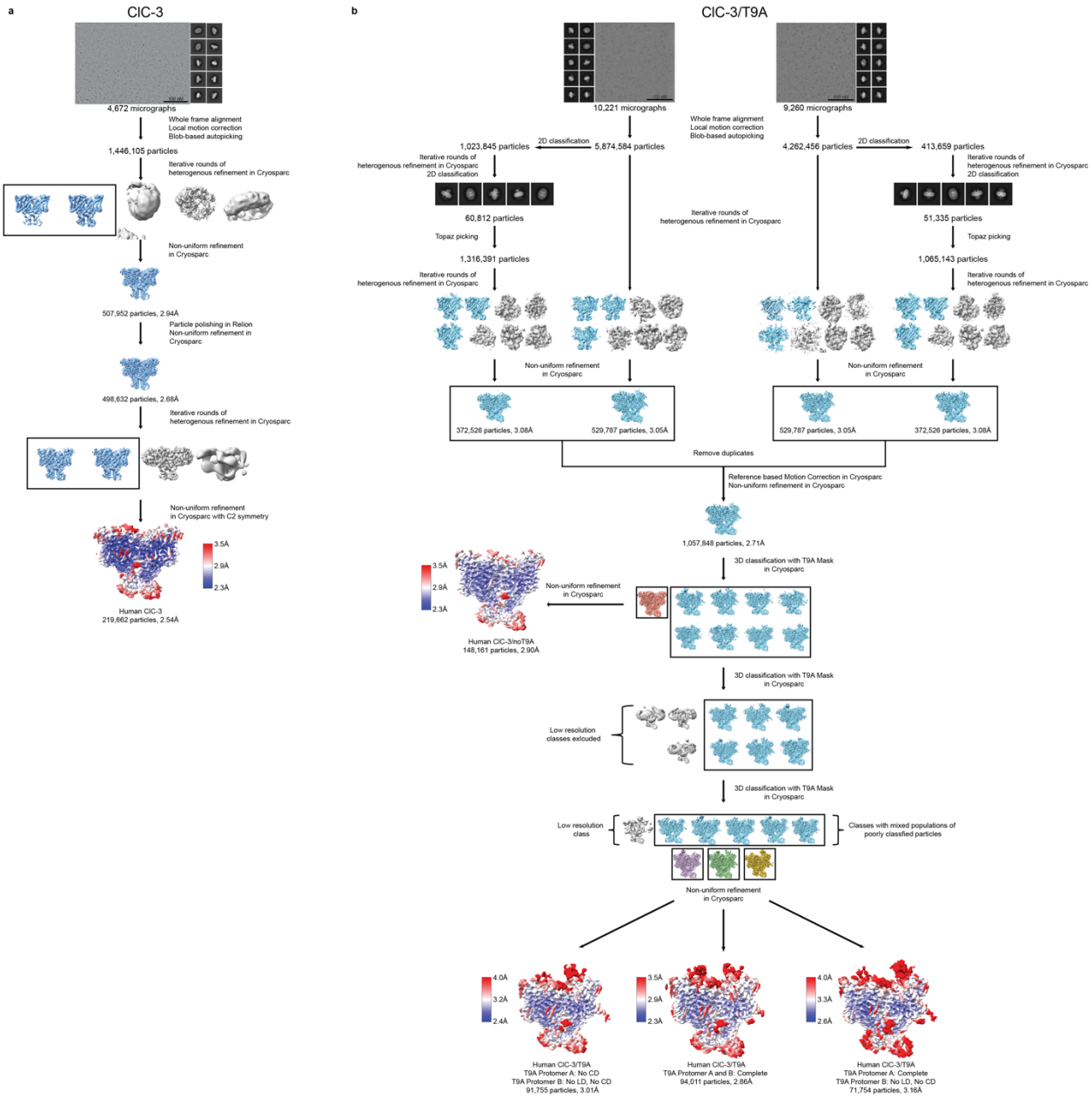

Extended Data Fig. 2: Cryo-EM analyses of ClC-3 (a) and ClC-3 in complex with T9A (b).

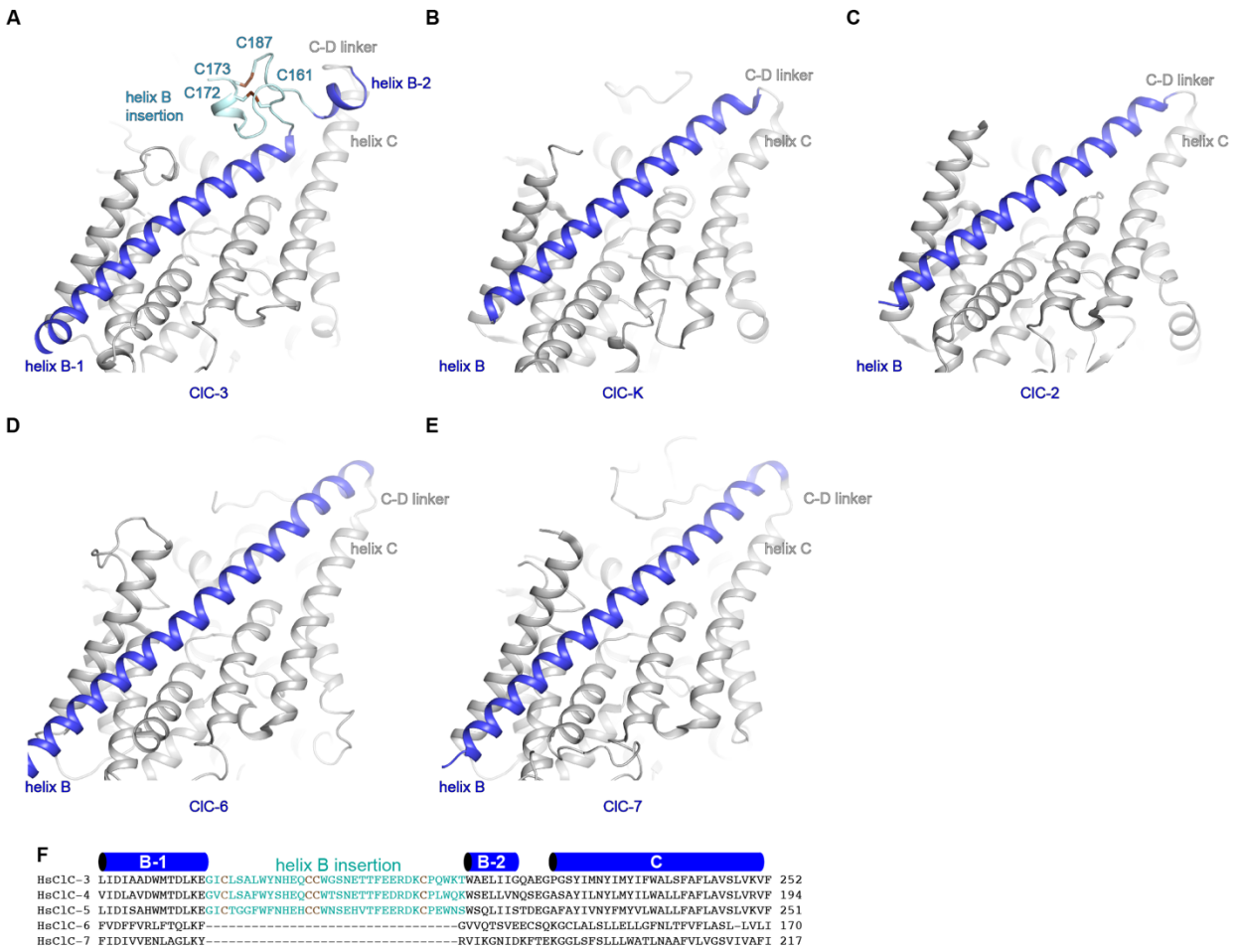

680

Extended Data Fig. 3: Conformation of helix B in mammalian CLC structures.
(**a-e**) Cartoon depiction of TMD of human ClC-3 (a), bovine ClC-K (b, PDB 5TQQ), human ClC-2 (c, PDB 8TA4), human ClC-6 (d, PDB 8JPJ) and human ClC-7 (e, PDB 7JM7). Helix B is colored in blue, the helix B insertion in ClC-3 is colored in light blue and all other residues are
685 colored in grey. Residues in ClC-3 that form disulfide bonds are shown as sticks.
(**f**) Sequence alignment of helix B of human ClC-3, ClC-4, ClC-5, ClC-6, and ClC-7. Secondary structural elements and residues that form disulfide bonds in ClC-3 are highlighted.

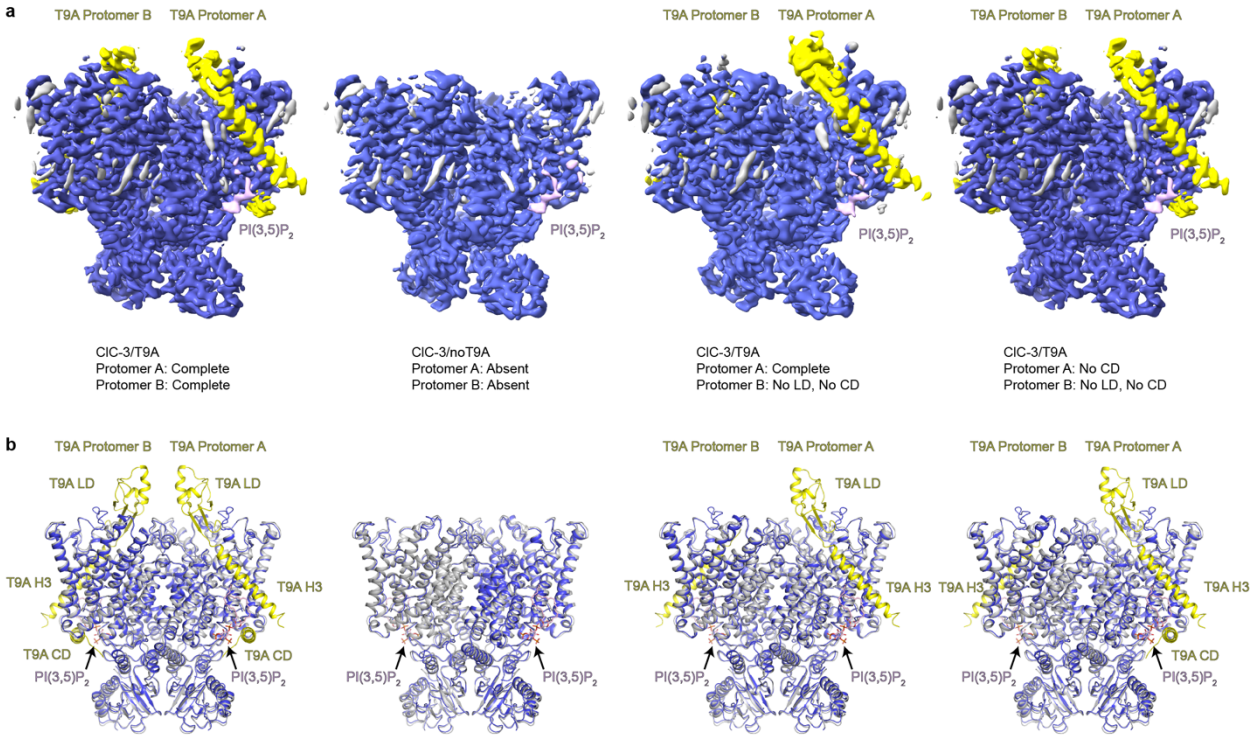

690

Extended Data Fig. 4: Structures of ClC-3 in the presence of T9A.

(**a**) Cryo-EM maps of ClC-3/T9A, ClC-3/noT9A and two classes of ClC-3 in complex with T9A in which the T9A protomers are only partially ordered, colored by subunit. Densities corresponding to ClC-3 are colored blue, T9A are colored yellow and $PI(3,5)P_2$ are colored pink.

695 (**b**) Superposition of ClC-3 alone (grey) with ClC-3/T9A, ClC-3/noT9A and two classes of ClC-3 in complex with T9A in which the T9A protomers are only partially ordered (colored by subunit).

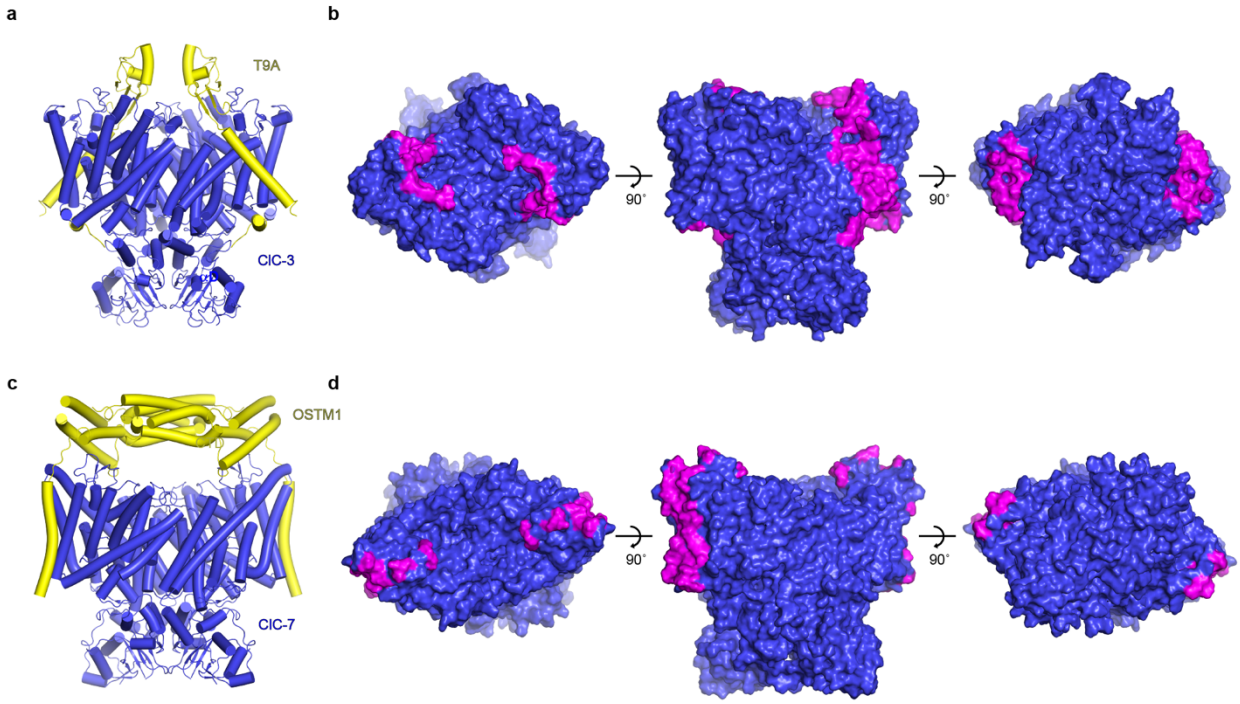

Extended Data Fig. 5: Comparison of ClC-3/T9A and ClC-7/OSTM1 complexes.
(**a,c**) Structures of ClC-3/T9A (a) and ClC-7/OSTM1 (c, PDB: 7JM7), colored by subunit. (**b,d**) Surface representation of ClC-3 (b) and ClC-7 (d), viewed from the cytosol (left), from within the plane of the membrane (middle) and lumen (right). Residues that interact with T9A or OSTM1 are colored in magenta.

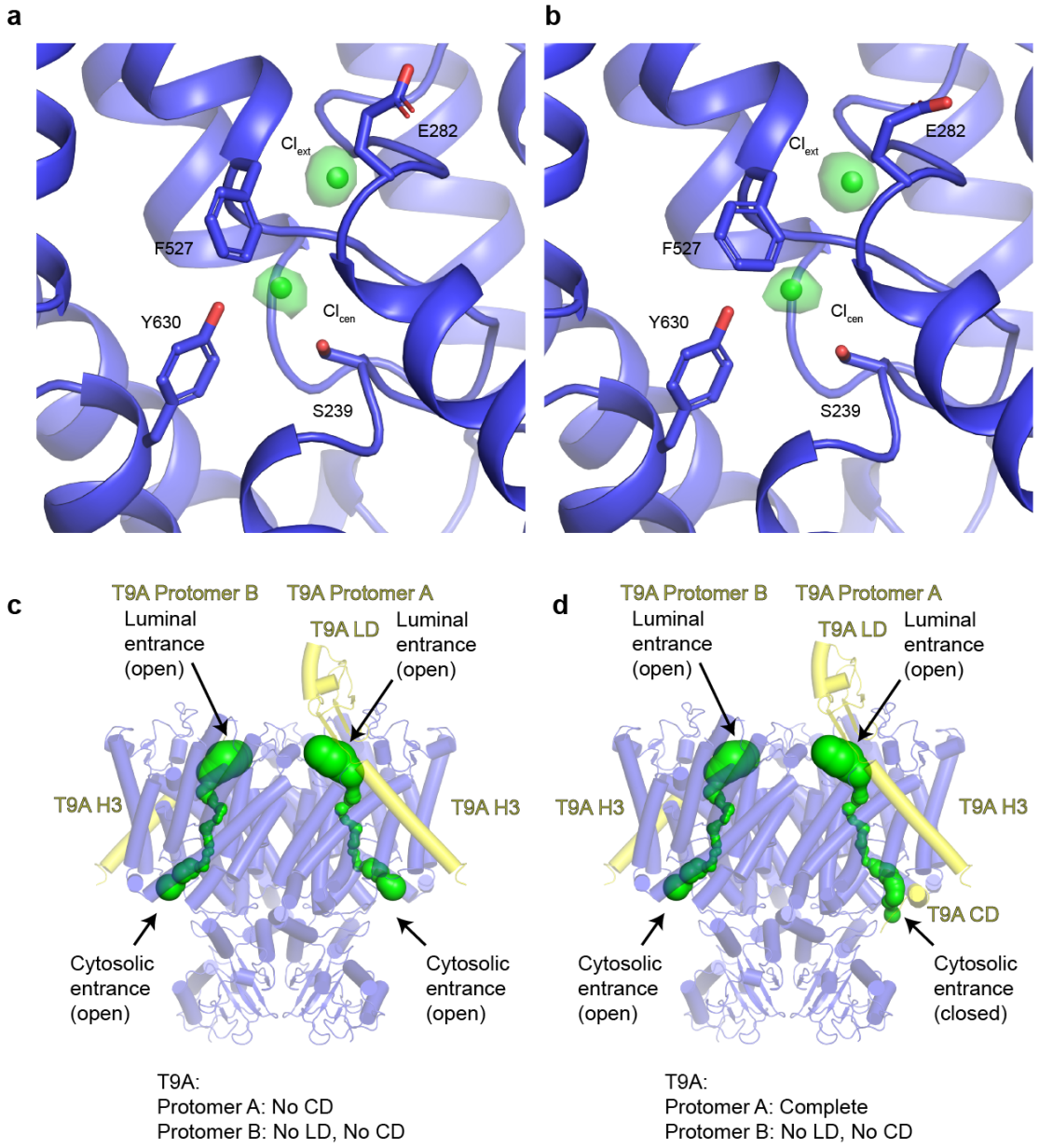

Extended Data Fig. 6: Cl^- ion pathway of ClC-3 in the presence of T9A.

(**a-b**) Cl^--binding sites in the Cl^- ion pathway of one protomer of ClC-3/T9A (a) or ClC-3/noT9A (b). Densities are shown as green isosurfaces and contoured at 4.0 s.

(**c-d**) Cl^- ion pathways of two classes of ClC-3 in complex with T9A in which the T9A protomers are only partially ordered, depicted as green surfaces.

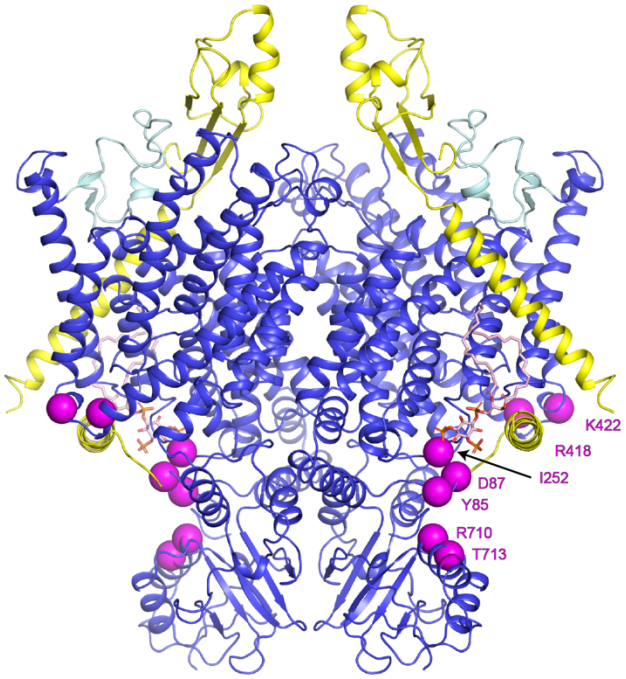

Extended Data Fig. 7: Disease-associated mutations in ClC-3/T9A. Residues whose mutation are associated with disease and weaken transport inhibition by T9A [28] are depicted as magenta spheres.

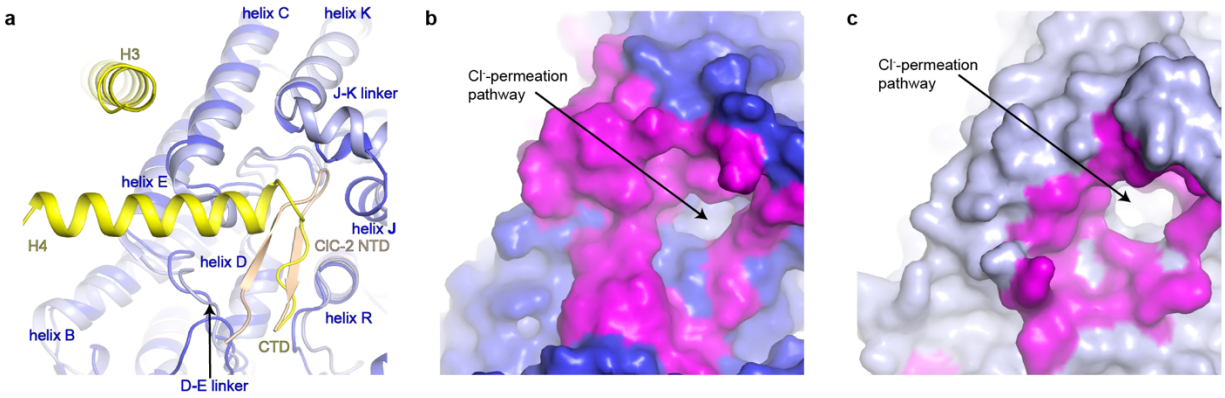

Extended Data Fig. 8: Comparison of ClC-3/T9A and ClC-2.

(**a**) Superposition of the region surrounding of the cytosolic entrances to the Cl^- ion pathways of ClC-3/T9A and ClC-2 (PDB 8TA4). ClC-3 is colored blue, T9A is colored yellow, ClC-2 is colored light blue, and the ClC-2 NTD is colored sand.

(**b-c**) Surface representation of the region surrounding the cytosolic entrances to the Cl^- ion pathways of CLC3 (b) and ClC-2 (c), with residues that interact with T9A or the N-terminus of ClC-2 colored in magenta.

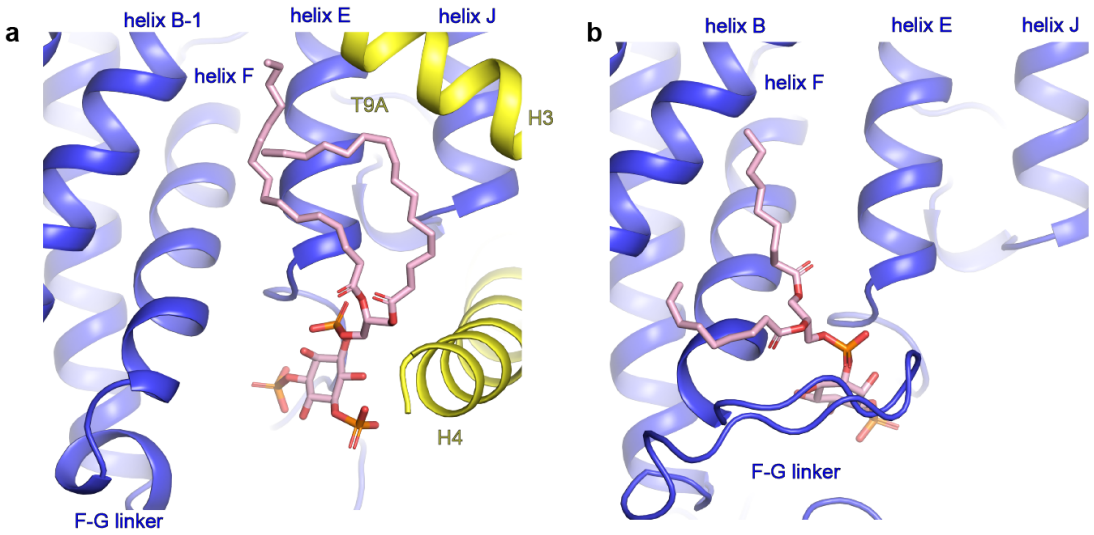

Extended Data Fig. 9: Phosphatidylinositol binding sites in ClC-3/T9A and ClC-7/OSTM1.
(**a**) PI(3,5)P_2 binding site in ClC-3/T9A.
(**b**) PI(3)P binding site in ClC-7/OSTM1 (PDB 7JM7).

	#1 ClC-3 (EMD-47070) (PDB 9DO0)	#2 ClC-3/noT9A (EMD-47066) (PDB 9DNW)	#3 ClC-3/T9A T9A Protomer A and B: Complete (EMD-47067) (PDB 9DNX)	#4 ClC-3/T9A T9A Protomer A: No CD T9A Protomer B: No LD, No CD (EMD-47068) (PDB 9DNY)	#5 ClC-3/T9A T9A Protomer A: Complete T9A Protomer B: No LD, No CD (EMD-47069) (PDB 9DNZ)
Data collection and processing					
Detector	Gatan K3	TFS Falcon4i	TFS Falcon4i	TFS Falcon4i	TFS Falcon4i
Magnification	29,000X	165000X	165000X	165000X	165000X
Voltage (kV)	300	300	300	300	300
Energy filter slit width (eV)		10	10	10	10
Electron exposure (e–/Å^2)	66	59.63	59.63	59.63	59.63
Defocus range (μm)	-0.7 to -2	-0.5 to -1.5	-0.5 to -1.5	-0.5 to -1.5	-0.5 to -1.5
Super-resolution pixel size (Å)	0.413				
Final pixel size (Å)	0.826	0.725	0.725	0.725	0.725
Symmetry imposed	C2	C2	C2	C1	C1
Initial particle images (no.)	1,446,105	10,137,040	10,137,040	10,137,040	10,137,040
Final particle images (no.)	219,662	148,161	94,011	91,755	71,754
Map resolution (Å) FSC threshold	2.54 0.143	2.90 0.143	2.86 0.143	3.01 0.143	3.16 0.143
Refinement					
Model resolution (Å) 0.5 FSC threshold	2.51	2.79	2.84	2.96	3.13
Map sharpening *B* factor (Å^2)	-30	-30	-30	-30	-30
Model composition	11,130	11,208	13,280	12,326	12,524

Non-hydrogen atoms Protein residues Ligands	1,394 8	1,399 10	1,656 10	1,540 10	1,562 10
Mean *B* factors (Å^2) Protein Ligand Water	58.0 52.1 26.4	26.1 15.5	67.4 52.3	46.0 35.2	63.8 53.3
R.m.s. deviations Bond lengths (Å) Bond angles (°)	0.002 0.426	0.002 0.449	0.003 0.477	0.002 0.476	0.002 0.499
Validation MolProbity score Clashscore Poor rotamers (%)	1.07 2.83 0.09	1.24 4.54 1.03	1.41 5.35 1.43	1.40 5.96 1.24	1.35 5.34 1.22
Ramachandran plot Favored (%) Allowed (%) Disallowed (%)	98.48 1.52 0.00	98.48 1.52 0.00	98.77 1.23 0.00	98.95 1.05 0.00	98.44 1.56 0.00

Extended Data Table 1. Cryo-EM data collection and refinement statistics.